Strain-induced formation of carbon and boron clusters in boron carbide during dynamic indentation

Dipankar Ghosh and Ghatu Subhash[a)]
Department of Mechanical and Aerospace Engineering, University of Florida, Gainesville, Florida 32611-6250

Chee Huei Lee and Yoke Khin Yap
Department of Physics, Michigan Technological University, 1400 Townsend Drive, Houghton, Michigan 49931-1295

The authors found that the level of amorphization or structural disorder in boron carbide is higher when induced by dynamic indentation compared to static indentation. Visible and uv Raman spectroscopies indicate that sp^2-bonded aromatic carbon clusters were formed, consistent with the detected photoluminescence spectra. Infrared absorption shows that amorphous boron clusters were created by dynamic indentation which has strain rates $\sim10^8$ order higher than that introduced by static indentation. The decreased intensity of infrared stretching mode of carbon-boron-carbon (CBC) chains also suggests that amorphization is due to the collapse of $B_{11}C(CBC)$ unit cells, which reorganize into the energetically favorite carbon and boron clusters. © *2007 American Institute of Physics*. [DOI: 10.1063/1.2768316]

Polycrystalline boron carbide (B_4C) exhibits localized amorphization due to local collapse of crystal structure under high contact pressure experiments.[1–4] Raman spectroscopic and temperature coefficient measurements of Raman bands on the nanoindented regions of single crystal B_4C suggested the presence of aromatic rings, containing sp^2 hybridized carbon (C) within amorphous B_4C (a-B_4C) along with boron (B) atoms present either as B clusters or within aromatic rings.[4] Fanchini *et al.*[5] stated that amorphization in B_4C may trigger from the collapse of $B_{12}(CCC)$ polytype instead of $B_{11}C(CBC)$, and a-B_4C may contain some segregated mixture of amorphous carbon (a-C) and boron icosahedrons (B_{12}). But any experimental evidence of a-C and B_{12} within a-B_4C is still lacking. Also, B_4C is generally accepted to have $B_{11}C(CBC)$ polytype instead of $B_{12}(CCC)$.[6,7] Therefore, the exact mechanism of B and C cluster formation within a-B_4C is unclear. Based on a series of microspectroscopic studies, including Raman (both uv and visible), photoluminescence (PL), and Fourier transformed infrared (FTIR) spectroscopy on the indented regions, we provide evidence for the formation of a-C and a-B clusters in B_4C.

It was earlier shown[2] through visible Raman spectroscopy that a-B_4C exists within the damaged regions beneath static and dynamic indentations of a polycrystalline B_4C. For static indentation, indentation load is transferred within 15 s (at a strain rate of 10^{-5}/s) whereas in dynamic indentation[8] load is delivered within $100-200$ μs (at a strain rate of 10^3/s). These damaged regions were probed using (i) visible Raman (He–Ne laser, 632.8 nm, 1.96 eV), (ii) uv Raman (He–Cd laser, 325 nm, 3.80 eV), (iii) photoluminescence (He–Cd laser, 325 nm, 3.80 eV), and (iv) FTIR spectroscopy in a reflection mode under a microscope with a focusing diameter of ~10 μm, close to the diffraction limit of infrared wavelengths.

Figures 1(a) and 1(b) show the visible Raman spectra collected from the unindented polished surface and damaged regions of static and dynamic indentations. For the unindented area, see Figs. 1(a) and 1(b), characteristic Raman peaks of B_4C structure[4,6,7] are detected within $200-1200$ cm^{-1}. A weak graphite (G) peak, around 1575 cm^{-1}, is attributed to the presence of small amount of free C associated with the unindented polycrystalline B_4C.[2] Static indented regions exhibited similar spectra with a distinct disorder-induced (D) peak (~1335 cm^{-1}) [see Figs. 1(a) and 1(b)]. The G and D peaks represent zone center phonons of E_{2g} symmetry and K-point phonons of A_{1g} symmetry of graphitic C, respectively.[9,10] The G peak is associated with in-plane bond-stretching motion of pairs of sp^2-bonded C atoms present either in olefinic chains or in aromatic rings whereas the D peak corresponds to the breathing mode of aromatic rings.

Significant changes were detected for dynamically indented regions [see Fig. 1(a)]. Intense G and D peaks were detected around 1590 and 1335 cm^{-1}, respectively. The evolution of these peaks for both type of indentations clearly suggest the formation of sp^2 hybridized aromatic C rings, indicating localized amorphization in B_4C.[2–4] Also, the stronger G and D peaks induced by dynamic indentation suggests a higher level of structural damage or amorphization in B_4C, as compared to static indentation.[2] This interpretation is also associated with the lower Raman shift of the characteristic breathing modes of the icosahedral $B_{11}C$ structures[4,6,7] of crystalline B_4C at ~1082 cm^{-1} (for dynamic indentation) and at ~1089 cm^{-1} (for static indentation) due to the strain induced by the amorphization.

Similar features were observed in uv Raman spectra, see Fig. 1(c), except that the two low frequency peaks of visible Raman spectra in the range from 250 to 350 cm^{-1} were absent. The origin of these two peaks is not well understood although they often appear in B_4C ceramics.[6] In addition, the ratio of intensities of D peak to that of G peak, i.e., I_D/I_G is ~0.6 for uv Raman and is ~1.1 for visible Raman. The

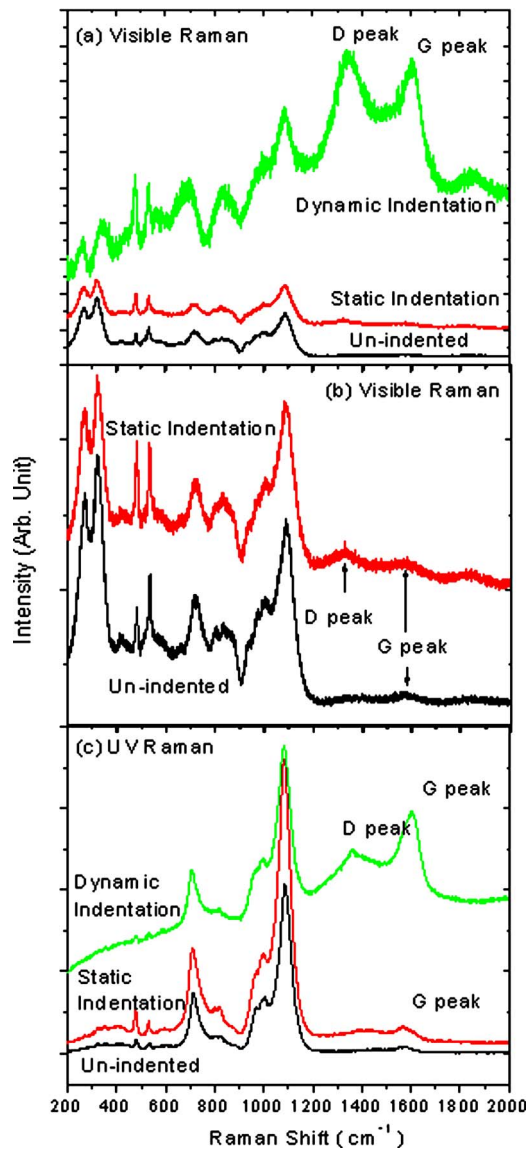[a)]Author to whom correspondence should be addressed; electronic mail: subhash@ufl.edu

FIG. 1. (Color online) (a) Visible Raman spectra and (c) uv Raman spectra from the unindented surface and damaged regions beneath the static and dynamic indentations. (b) Magnified view of two of the spectra in (a).

FIG. 2. (Color online) Photoluminescence from the unindented surfaces and damaged regions beneath the static and dynamic indentations.

observed I_D/I_G values and their deviation (i.e., dispersion) are similar to that detected from hydrogenated and nonhydrogenated a-C films with sp^2-bonded C clusters.[11,12] Also, D peak disappears under uv excitation for disordered and nanocrystalline graphite but not for a-C.[12] Besides, diamond-like carbon films with predominated sp^3-bonded C usually have low I_D/I_G values (<0.3) and low I_D/I_G dispersion (<0.3), suggesting a low sp^3 hybridized C content in the a-C formed within the indented regions. Therefore, Raman spectroscopy confirmed the formation of sp^2-bonded aromatic C clusters by static and dynamic indentations due to amorphization of B_4C. Also, dynamic loading results in a greater level of C cluster formation compared to static loading. This is also supported from the dispersion of G peak to higher frequency in the visible [Fig. 1(a)] and uv Raman spectra [Fig. 1(c)] for dynamic indentation compared to the static indentation.[12,13]

Figure 2 presents the PL spectra of B_4C obtained from the unindented surface and the indented regions of static and dynamic indentations. For unindented surface, a weak PL band at 2.4 eV was 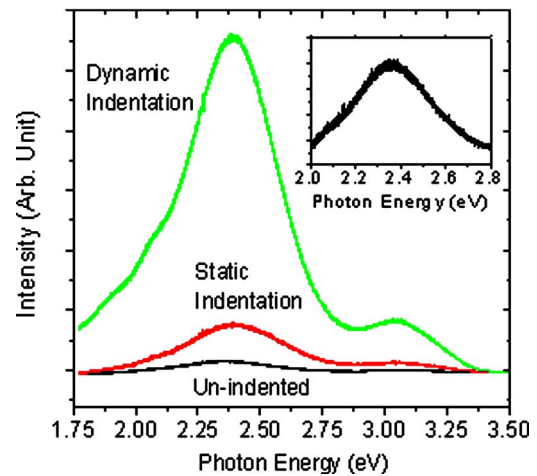detected and became stronger for static indentation and strongest for dynamic indentation. A shoulder peak at ~ 2.05 eV was observed for all the spectra (inset is for unindented regions only). Both type of indented regions exhibited another peak at ~ 3.05 eV which was again stronger under dynamic indentation compared to static indentation. The PL band at ~ 2.05 eV is associated with the optical band gap of B_4C.[14] The other two PL signals (at ~ 2.4 and ~ 3.05 eV) are not associated with B_4C as they appear well above the optical band gap and their origin is explained as follows. Amorphous carbon (a-C) and hydrogenated a-C (a-C:H) films exhibit a broad PL band from ~ 1.8 to 3.7 eV.[15] These films contain sp^2-bonded C clusters embedded within a-C matrix. Their band gaps depend on the size and distribution of the sp^2 C clusters. Since Raman spectra indicated a-C structures within the indented regions, we rationalize that the PL spectra detected here are attributed to radiative recombination mechanism of photoexcited electrons and holes in localized tail states within sp^2 C clusters.[15] Similar to Raman spectra, PL results also indicate the presence of more aromatic sp^2 C clusters within dynamically indented regions.

To further clarify the structure of a-B_4C, FTIR spectra were collected from unindented and indented areas (see Fig. 3). All these peaks are similar (except one to be discussed later) and characteristic of crystalline B_4C. The FTIR peak at
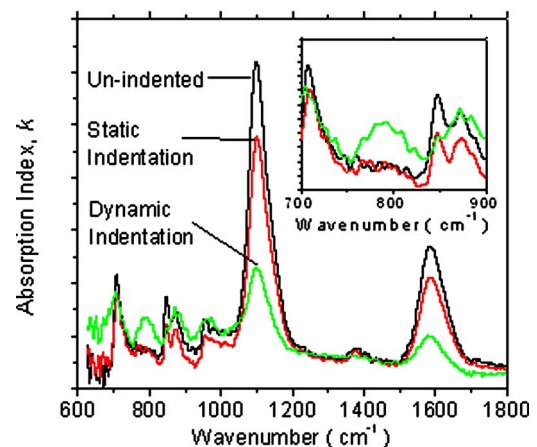

FIG. 3. (Color online) FTIR spectra from the unindented surfaces and damaged regions beneath the static and dynamic indentations.
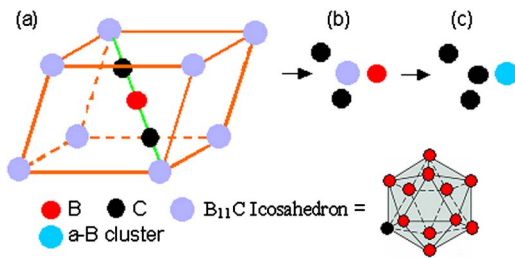
FIG. 4. (Color online) Schematic of (a) a rhombohedral unit cell of B_4C with eight $B_{11}C$ icosahedrons at the corners. (b) Amorphization of each unit cell will form two carbon and one boron atoms and a $B_{11}C$ icosahedron. (c) One $B_{11}C$ icosahedron and one boron atom will reorganize into one amorphous boron ($a-B$) cluster and a carbon atom that form carbon clusters with adjacent carbon.

~ 1100 cm^{-1} corresponds to the B–C stretching vibration whereas the peak around 1590 cm^{-1} originates from the stretching of CBC chains[16] present along one of the body diagonals of the rhombohedral unit cell of B_4C (Ref. 6) [see Fig. 4(a)]. The intensities of these peaks gradually decrease in succession from the unindented surface to static to dynamic indentations. This trend clearly indicates structural distortion in B_4C during indentation. Decreased intensity of FTIR peaks from static to dynamic indentations suggests a greater amorphization or structural disorder. The only difference was the appearance of an infrared (IR) band between ~ 760 and 830 cm^{-1} (shown in the inset) for dynamic indentation. This peak covers the known IR signal for free icosahedral B_{12} molecules.[17,18] Due to its broad distribution, it is more appropriate to assign this IR band to amorphous B clusters, in consistent with a reported data.[18] Therefore, FTIR clearly suggests the formation of a-B clusters within the a-B_4C created by dynamic indentation although no such evidence was observed in the FTIR spectrum for static indentation.

Finally, we present a schematic of the formation of a-C and a-B clusters. B_4C has a rhombohedral unit cell with eight $B_{11}C$ icosahedrons at the corners [see Fig. 4(a)]. Amorphization causes each unit cell to collapse into two C atoms, one B atom, and a $B_{11}C$ icosahedron [Fig. 4(b)]. The possible mechanism could have been accompanied by the col-

lapse of $B_{11}C$ icosahedron, which may be energetically more stable to release the C atom and replace with a B atom. This reorganizes into one a-B_{12} cluster and one C atom to form C clusters with adjacent C atoms [Fig. 4(c)].

In summary, we have shown that a-C clusters are formed in the indented regions from Raman and PL spectroscopy. FTIR analysis reveals the existence of a-B clusters within the dynamically indented region.

[1]M. Chen, J. W. McCauley, and K. J. Hemker, Science **299**, 1563 (2003).
[2]D. Ghosh, G. Subhash, T. S. Sudarshan, R. Radhakrishnan, and X.-L. Gao, J. Am. Ceram. Soc. **90**, 1850 (2007).
[3]D. Ge, V. Domnich, A. Juliano, E. A. Stach, and Y. Gogotsi, Acta Mater. **52**, 3921 (2004).
[4]X. Q. Yan, W. J. Li, T. Goto, and M. W. Chen, Appl. Phys. Lett. **88**, 131905 (2006).
[5]G. Fanchini, J. W. McCauley, and M. Chhowalla, Phys. Rev. Lett. **97**, 035502 (2006).
[6]R. Lazzarari, N. Vast, J. M. Besson, S. Baroni, and A. D. Corso, Phys. Rev. Lett. **83**, 3230 (1999).
[7]I. Jimenez, D. G. J. Sutherland, T. v. Buuren, J. A. Carlisle, L. J. Terminello, and F. J. Himpsel, Phys. Rev. B **57**, 13167 (1998).
[8]G. Subhash, *ASM Handbook®, Mechanical Testing and Evaluation,* ASM Handbook vol. 8, (ASM International, Materials Park, Ohio, 2000), p. 519.
[9]Y. K. Yap, S. Kida, T. Aoyama, Y. Mori, and T. Sasaki, Appl. Phys. Lett. **73**, 915 (1998).
[10]Y. K. Yap, M. Yoshimura, Y. Mori, and T. Sasaki, Appl. Phys. Lett. **80**, 2559 (2002).
[11]M. Ramsteiner and J. Wanger, Appl. Phys. Lett. **51**, 1355 (1987).
[12]A. C. Ferrari and J. Robertson, Phys. Rev. B **64**, 075414 (2001).
[13]A. C. Ferrari and J. Robertson, Phys. Rev. B **61**, 14095 (2000).
[14]H. Werheit, J. Phys.: Condens. Matter **18**, 10655 (2006).
[15]J. Xu, J. Mei, X. Huang, W. Li, Z. Li, X. Li, and K. Chen, J. Non-Cryst. Solids **338–340**, 481 (2004).
[16]H. Werheit, T. Au, and R. Schmechel, J. Solid State Chem. **154**, 79 (1999).
[17]C. L. Beckel, M. Yousaf, M. Z. Fuka, S. Y. Raja, and N. Lu, Phys. Rev. B **44**, 2535 (1991).
[18]K. Shirai, S. Emura, S.-i. Gonda, and Y. Kumashiro, J. Appl. Phys. **78**, 3392 (1995).